

Identifying All Moiety Conservation Laws in Genome-Scale Metabolic Networks

Original

Identifying All Moiety Conservation Laws in Genome-Scale Metabolic Networks / De Martino, A.; De Martino, D.; Mulet, R.; Pagnani, Andrea. - In: PLOS ONE. - ISSN 1932-6203. - ELETTRONICO. - 9:(2014), p. e100750. [10.1371/journal.pone.0100750]

Availability:

This version is available at: 11583/2568339 since: 2016-02-18T13:45:54Z

Publisher:

Public Library of Science

Published

DOI:10.1371/journal.pone.0100750

Terms of use:

This article is made available under terms and conditions as specified in the corresponding bibliographic description in the repository

Publisher copyright

(Article begins on next page)



Identifying All Moiety Conservation Laws in Genome-Scale Metabolic Networks

Andrea De Martino^{1,2,3*}, Daniele De Martino^{3,*}, Roberto Mulet⁴, Andrea Pagnani^{5,6}

1 CNR-IPCF, Unità di Roma-Sapienza, Roma, Italy, **2** Dipartimento di Fisica, Sapienza Università di Roma, Roma, Italy, **3** Center for Life Nano Science@Sapienza, Istituto Italiano di Tecnologia, Roma, Italy, **4** Henri-Poincaré-Group of Complex Systems and Department of Theoretical Physics, Physics Faculty, University of Havana, La Habana, Cuba, **5** DISAT and Centre for Computational Sciences, Politecnico di Torino, Torino, Italy, **6** Human Genetics Foundation, Torino, Italy

Abstract

The stoichiometry of a metabolic network gives rise to a set of conservation laws for the aggregate level of specific pools of metabolites, which, on one hand, pose dynamical constraints that cross-link the variations of metabolite concentrations and, on the other, provide key insight into a cell's metabolic production capabilities. When the conserved quantity identifies with a chemical moiety, extracting all such conservation laws from the stoichiometry amounts to finding all non-negative integer solutions of a linear system, a programming problem known to be NP-hard. We present an efficient strategy to compute the complete set of integer conservation laws of a genome-scale stoichiometric matrix, also providing a certificate for correctness and maximality of the solution. Our method is deployed for the analysis of moiety conservation relationships in two large-scale reconstructions of the metabolism of the bacterium *E. coli*, in six tissue-specific human metabolic networks, and, finally, in the human reactome as a whole, revealing that bacterial metabolism could be evolutionarily designed to cover broader production spectra than human metabolism. Convergence to the full set of moiety conservation laws in each case is achieved in extremely reduced computing times. In addition, we uncover a scaling relation that links the size of the independent pool basis to the number of metabolites, for which we present an analytical explanation.

Citation: De Martino A, De Martino D, Mulet R, Pagnani A (2014) Identifying All Moiety Conservation Laws in Genome-Scale Metabolic Networks. PLoS ONE 9(7): e100750. doi:10.1371/journal.pone.0100750

Editor: Olivier Lespinet, Université Paris-Sud, France

Received: March 17, 2014; **Accepted:** May 26, 2014; **Published:** July 2, 2014

Copyright: © 2014 De Martino et al. This is an open-access article distributed under the terms of the Creative Commons Attribution License, which permits unrestricted use, distribution, and reproduction in any medium, provided the original author and source are credited.

Funding: Work was supported by the DREAM Seed Project of the Italian Institute of Technology (IIT) and by the joint IIT/Sapienza Lab "Nanomedicine". The funders had no role in study design, data collection and analysis, decision to publish, or preparation of the manuscript.

Competing Interests: The authors have declared that no competing interests exist.

* Email: daniele.demartino@roma1.infn.it

These authors contributed equally to this work.

Introduction

When studying metabolic networks at the scale of the whole genome, it is often the case that the information required to develop dynamical models is not available, because either kinetic parameters or reaction mechanisms are partially or fully unknown. In many cases, the most reliable information is encoded in the stoichiometry of the reaction network (the stoichiometric matrix) and, partly, in the assignment of reaction reversibility [1–4]. Based on these, constraint-based models like Flux Balance Analysis (FBA) have been able to shed light on functional optimality in different contexts, providing (mostly for unicellular organisms) unprecedented predictive power on issues like the organization of reaction fluxes, response to knock-outs, or gene essentiality [5–8]. FBA can now almost routinely be performed on genome-scale networks [9]. Stoichiometric matrices however harbor a host of additional physical, biological and functional information [5,10–12], including regulatory (see e.g. extreme pathways [13,14] and flux modes [15]), robustness (see e.g. the geometry of the FBA solution space [16–18]) and statistical (see e.g. the individual distributions of allowed fluxes and flux-flux correlations [18–20]) characterizations. Unluckily, the full solution of the problems just listed on genome-scale networks with thousands of reactions and metabolites presents serious computational challenges, as the algorithms

currently available do not scale gently with the system size. This is also the case for the identification of moiety conservation laws that we shall consider here [10,21,22].

Conservation relationships for concentration variables emerge in biochemical reaction networks from the sheer structure of their input-output stoichiometry [10]. In particular, given a stoichiometric matrix, it is generically possible to find linear combinations of metabolite levels that are due to be constants of motion of the dynamical system governing the time evolution of concentrations and reaction rates. For instance, if the subset of metabolic reactions describing energy metabolism is considered, ATP and ADP would be coupled in every reaction – one is a product whenever the other is a substrate –, so that the aggregate concentration of ATP and ADP would remain constant over time while individual levels may fluctuate in a correlated way. The existence of such relationships has profound consequences. In first place, any intervention aimed at altering the level of a certain metabolite should consider whether its variations are limited or not by conservation laws. Secondly, conservation laws constrain a network's production capabilities, as there clearly cannot be a net stationary output of a compound belonging to a conserved quantity. Therefore, mapping out these conservation laws amounts to obtaining a genome-scale picture of what a cell can (in principle) excrete or make available to processes outside

metabolism, in particular secondary metabolism, e.g. the production of pigments and antibiotics. Finally, conserved quantities imply an effective reduction of the number of independent flux or concentration variables in a reaction network, an important aspect especially for dynamical modeling.

The problem of finding generic conservation laws is relatively straightforward to solve with the tools of linear algebra, since, as said above, they correspond to specific (linear) dependencies of the rows of the stoichiometric matrix. When one is interested in the conservation of particular chemical moieties, however, the problem takes a more challenging twist. Indeed, because of intrinsic discreteness, the combinations that describe moiety conservation should only be constructed with non-negative integers. We refer to these particular combinations as ‘moiety conservation laws’ (MCLs), and we shall be interested in finding a basis for MCLs (i.e. a maximal linearly independent set of MCLs) in large, genome-scale metabolic networks. Computing an MCL basis in a large system is much harder than finding linear row-dependencies, as one passes from a linear to an integer-linear programming problem with the concomitant increase of computational complexity up to NP-hard [23,24]. On the other hand, knowledge of an MCL basis allows, as we shall see, to map out exhaustively a large class of conservation laws in biochemical networks.

The literature on conservation laws in reaction networks, mostly focused on characterizing the so-called semi-positive conservation laws (SPCLs, given by linear combinations of MCL basis vectors), is quite rich. Pioneering mathematical analyses of SPCLs in biochemical systems date back to the early 1990’s [21,25]. Besides clarifying the origin and significance of these invariants, such studies have shown that conservation laws can be encoded in a convex representation of the left kernel of the stoichiometric matrix [25]. Later on [22], a classification of conservation laws has been proposed based on an analogy between properties of the right (extreme pathways) and left null spaces of the stoichiometric matrix. The computational demand of finding MCLs in genome-scale networks has driven further work concerned with the development of *ad hoc* algorithms [26,27]. After the seminal proposals made in [25], already in [22] a method is presented, that however scales exponentially with the system size and can only be employed for the analysis of rather small networks. The Metabolite Concentration Coupling Analysis (MCCA) and the Minimal Pool Identification (MPI) tools for genome-scale metabolic network analysis were instead introduced in 2005 [28]. The former allows for the identification of subsets of metabolites whose concentrations are coupled within common SPCLs, while MPI helps to determine the SPCLs for individual metabolites. More recently [29], the formal algebraic duality of metabolite producibility and conservation has been exploited to devise a method that relates biomass producibility to nutrient availability, which was then applied to the metabolism of *Escherichia coli*, obtaining a large set of novel putative growth media. Then in [30] a mixed integer-linear programming problem has been posed and solved in order to find the ensemble of all metabolites that appears in SPCLs. Furthermore, in modeling metabolic networks in terms of Petri nets, the problem of finding MCLs has been connected with the search for the so-called P-invariants of the network [31]. It is worth noting that metabolite levels are in principle experimentally accessible (e.g. by mass spectrometry), although such knowledge is mostly used in metabolomic analysis to reconstruct flux patterns.

Despite many efforts, a consistent computational method to determine *all* MCLs in genome-scale networks has remained so far elusive. In this work we construct such a computational method. The technique we propose exploits the above mentioned duality

and combines different kinds of algorithms (message passing, Monte Carlo and relaxation). The mathematical background and the structure of the method we employ are discussed in ‘Materials and Methods’. As case studies, we have considered different reconstructions of the metabolic network of the bacterium *E. coli* and six tissue-specific human metabolic networks derived from the Recon-2 database [32]. In particular, we have been able to identify in each case *all* MCLs in different conditions (see ‘Results’). Furthermore, by studying *E. coli* we have uncovered a relation between the number of pools and the size of a network (number of metabolites and/or reactions), a theoretical justification for which is also discussed, before reporting our conclusions.

Materials and Methods

Methods

Background. Given a metabolic network encoded by the stoichiometric matrix $\mathbb{S}=(S_{mr})$, where S_{mr} is the stoichiometric coefficient of metabolite $m \in \{1, \dots, M\}$ in reaction $r \in \{1, \dots, N\}$ (with the standard sign convention to distinguish substrates from products), the time evolution of the concentration vector $\mathbf{c}=\{c_m\}$ satisfies

$$\dot{\mathbf{c}}=\mathbb{S}\mathbf{v}, \quad (1)$$

where $\mathbf{v}=\{v_r\}$ is the vector of reaction fluxes and we have assumed that the stoichiometry of metabolite exchanges with the environment is included in \mathbb{S} . Consider a linear combination Q of concentration variables with fixed coefficients $k_m \geq 0$, i.e.

$$Q=\sum_{m=1}^M k_m c_m \equiv (\mathbf{k}, \mathbf{c}), \quad \mathbf{k}=\{k_1, \dots, k_M\}, \quad (2)$$

where the bracket (\cdot, \cdot) stands for the scalar product. Clearly,

$$\dot{Q}=(\mathbf{k}, \dot{\mathbf{c}})=(\mathbf{k}, \mathbb{S}\mathbf{v})=(\mathbf{v}, \mathbb{S}^T \mathbf{k}). \quad (3)$$

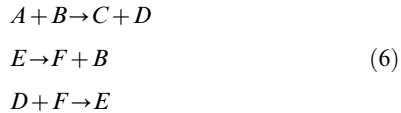
So if \mathbf{k} belongs to the left null-space of \mathbb{S} , that is if

$$\mathbb{S}^T \mathbf{k}=\mathbf{0}, \quad \mathbf{k} \neq \mathbf{0}, \quad k_m \geq 0 \quad \forall m \in \{1, \dots, M\} \quad (4)$$

then the aggregate concentration variable Q is conserved in *any* flux state \mathbf{v} . Following [21], we shall generically call a conserved metabolite pool like Q , defined by a vector \mathbf{k} satisfying (4), a ‘semi-positive conservation law’ (SPCL). From a physical viewpoint, a SPCL represents an invariance constraint that is required to be satisfied by trajectories of the dynamics of the system, i.e. by solutions of (1) with given specifications of how \mathbf{v} depends on \mathbf{c} . In principle, every vector \mathbf{k} belonging to the left kernel of \mathbb{S} (without sign restriction) defines a conserved quantity, to which we can refer generically as a ‘conservation law’. The total number of linearly independent conservation laws of this type equals the dimension of the left null-space of \mathbb{S} , i.e. $M-\text{rank}(\mathbb{S})$. This number also provides an upper bound to the number of linearly independent SPCLs, namely

$$\#\{\text{independent SPCLs}\} \leq M-\text{rank}(\mathbb{S}). \quad (5)$$

The restriction to $\mathbf{k} \geq \mathbf{0}$ in (4) allows for a more straightforward interpretation of quantities like Q . Considering, for instance, the toy network formed by the three reactions



a simple calculation shows that two conserved quantities exist, i.e. $Q_1 = c_B + c_E + c_D$ and $Q_2 = c_E + c_F$. However, Q_2 could be also written as $Q_2 = c_F - c_B - c_D$. While both Q_1 and Q_2 are conserved quantities, Q_1 can be interpreted to be a total enzyme mass if E and F represent, respectively, a bound and a free enzyme species. A similar physical interpretation is harder to imagine for Q_2 (and the situation rapidly becomes more complicated in larger networks).

Among solutions of (4), those for which the coefficients k_m are *non-negative integers* can be fully rationalized in chemical terms as related to the conservation of moieties, groups or chemical elements. We shall hereafter define a ‘moiety conservation law’ (MCL) as a solution of

$$\mathbb{S}^T \mathbf{k} = \mathbf{0}, \quad \mathbf{k} \neq \mathbf{0}, \quad k_m \in \mathbb{N} \equiv \{0, 1, 2, \dots\} \forall m. \tag{7}$$

The problem we face here concerns the identification of all MCLs of a given stoichiometric matrix \mathbb{S} . Furthermore, we will be interested in constructing an integer basis of the left null space of \mathbb{S} through which all SPCLs can be obtained as linear combinations with real coefficients. From a mathematical view point, finding such a basis represents a variation of the more general problem of computing the minimal integer Hilbert basis of the polyhedral cone defined by the left null-space of the stoichiometric matrix, which is known to be NP-hard [33,34]. Although some exact deterministic algorithms are available [35,36], their computational costs become too high when the underlying network is sufficiently large. In particular, for the sizes relevant to genome-scale metabolic modeling ($N, M \gtrsim 10^3$) one always runs into the combinatorial explosion of computation times.

Incidentally, if this integer basis suffices to generate all conservation laws via linear combinations with real coefficients, then all conservation relationships encoded in \mathbb{S} are SPCLs and the number of MCLs in the basis saturates the bound (5). Otherwise, \mathbb{S} necessarily allows for at least one conservation law that cannot be expressed through a SPCL but also involves negative coefficients. In such cases, we have $\#\{\text{independent MCLs}\} < M - \text{rank}(\mathbb{S})$ and an integer basis of the left kernel, rigorously speaking, does not exist.

It is very important to stress that a high computational complexity does not necessarily imply the existence of an exponential number of elements of the MCL basis (as a matter of fact, we shall see that the basis size grows roughly linearly with the network size); rather, it quantifies the time required to find a single element of the basis in the worst case. Roughly speaking, combinatorial explosion of computing times occurs when one has to go through an exponential number of candidates (\mathbf{k} -vectors in our case) before finding a solution of (7). It is rather intuitive that finding all solutions of (7) by a deterministic procedure would require exploring the entire space of \mathbf{k} -vectors, which assuming non-zero upper bounds for the k_m 's is indeed exponentially large in the number of metabolites.

In order to find all independent solutions to (7), stochastic strategies are therefore mandatory. In brief, we shall map this task to a global optimization problem whose solution can be retrieved via stochastic algorithms known to be exact in special situations, a kind of approach that has been used before with considerable

success in the solution of other NP-complete and NP-hard problems [18,37–39]. Our strategy is divided in three steps: (a) compute a list of all metabolites belonging to at least one MCL; (b) construct an integer basis for MCLs from that list; (c) check that \mathbb{S} does not allow for any further MCL. Step (a) can be carried out in different ways, starting, as we shall see, from a straightforward analysis of the kernel of \mathbb{S}^T . We shall also discuss here a more involved but more informative approach based on a message-passing procedure. Step (b) will be done by Monte Carlo and step (c) by a relaxation algorithm. The conceptual implementation of each step is sketched below and a C++ code performing the complete procedure can be downloaded from <http://chimera.roma1.infn.it/SYSBIO/>, together with a test case (the *E. coli* iAF1260 network). Further details and work flow are given in the Text S1.

Step (a): finding all metabolites belonging to at least one MCL. A first, elementary preprocessing step may consist in computing the left kernel of \mathbb{S} , e.g. by Gaussian elimination. Evidently, every vector in a basis of $\text{Ker}(\mathbb{S}^T)$ is a generic, linearly independent conservation law, i.e. a non-null solution of $\mathbb{S}^T \mathbf{k} = \mathbf{0}$ with real-valued \mathbf{k} . Eventually, some of these vectors will be such that $k_m \geq 0$ for each m , i.e. will be outright SPCLs. The search for MCLs can be carried out among metabolites that appear in this basis with positive components. Furthermore, the size of such a basis is an upper bound for the maximum number of linearly independent MCLs. In order to compute the left kernel, we resort to a Gaussian elimination method with partial scaled pivoting, a technique currently employed to deal effectively with possible ill-conditioning of the stoichiometric matrix under control. We however cross-checked results, in every case, with the results obtained by the robust routines employed by both *Mathematica* and *MatLab* softwares. Ultimately, though, the relaxation algorithm discussed below provides a definitive certificate for correctness, in the sense that convergence only occurs when all kernel vectors have been found (and removed from the stoichiometric matrix, see below).

A more complex but (in our view) more rewarding alternative is suggested by the following considerations. Because MCLs are represented by solutions of (7), one could obtain a statistical picture of the set of MCLs by computing the marginals of the probability distribution

$$P(\mathbf{k}) = \frac{1}{\mathcal{N}_{\text{sol}}} \prod_{i=1}^N \delta \left(\sum_{m=1}^M S_{m,i} k_m; 0 \right), \quad k_m \in \mathbb{N} \quad \forall m, \tag{8}$$

where $\delta(x; y)$ is the Kronecker delta function ($= 1$ if $x = y$ and $= 0$ otherwise) and \mathcal{N}_{sol} stands for the number of solutions of (7). Indeed, each marginal

$$P_m(k_m) \equiv \sum_{\{k_n\}_{n \neq m}} P(\mathbf{k}) \tag{9}$$

represents the probability that the m -th component of the \mathbf{k} vector attains a value k_m over the solution space of (7). Disposing of all such marginals is equivalent to disposing of the list of metabolites belonging to at least one MCL, since $P_m(k_m) = 0$ implies that metabolite m does not belong to any MCL. Actually, the set of marginals provides much more information than that: in fact, by definition,

$$P_m(k_m) = \frac{1}{N_{\text{sol}}} \sum_{s=1}^{N_{\text{sol}}} \delta(k_m^s; k_m), \quad (10)$$

where in the last equivalence we stressed the probabilistic interpretation of the marginal as the histogram of the m -th coordinate over the solutions $\{\mathbf{k}^s\}$, $s=1, \dots, N_{\text{sol}}$. So, P_m is proportional to the number of distinct MCLs to which metabolite m belongs.

Unluckily, a direct evaluation of (10) requires computing a sum over k_{max}^{M-1} terms (assuming $k_m \in \{0, 1, 2, \dots, k_{\text{max}}\}$), which becomes computationally infeasible for M larger than a few tens. We can however estimate each marginal effectively by resorting to message-passing (MP) techniques. MP is an efficient computational strategy (with a running time scaling linearly, as opposed to exponentially, with the number of variables) that is formally exact on locally tree-like networks [40–42] and is extensively used as a heuristic procedure to solve hard computational problems defined on sparse or even loopy networks [37,43,44]. It has been also applied previously to the analysis of metabolic networks [18].

In short, we have devised a MP algorithm to compute the marginals (10) and obtain a full statistical representation of the space of MCLs. Details are given in the Text S1. Upon convergence, when all marginal probability distributions are evaluated, one disposes of a list of metabolites belonging to at least one MCL (with the additional information described above). The following step concerns the construction of an integer basis for MCLs from this list.

Step (b): constructing the basis. Because MP will have considerably pruned the set of metabolites (thereby greatly reducing the number of variables: we shall now denote by M_c the number of metabolites belonging to at least one MCL), the most convenient method to explore the structure of individual MCLs is Monte Carlo. Indeed, the problem of finding the integer solutions of (7) can be mapped onto that of finding the minima of the fictitious, discrete ‘energy function’ given by

$$E(\mathbf{k}) = \sum_{i=1}^N \left(\sum_{n=1}^{M_c} S_{m,i} k_n \right)^2 = \sum_{m,n=1}^{M_c} J_{m,n} k_m k_n \geq 0, \quad (11)$$

where $k_m \in \{0, 1, 2, \dots\} \forall m$ and

$$J_{m,n} \equiv \sum_{i=1}^N S_{m,i} S_{n,i}. \quad (12)$$

Note that $E(\mathbf{k})=0$ if \mathbf{k} satisfies (7). Therefore MCLs correspond to the minima of E . Several controlled and optimized Monte Carlo methods are available to compute the minima of functions like (11) [45]. More specifically, these protocols (the simplest of which is probably the Metropolis scheme) are capable of sampling vectors \mathbf{k} distributed according to

$$P(\mathbf{k}) = \frac{e^{-E(\mathbf{k})/T}}{Z(T)}, \quad (13)$$

where $T > 0$ is a parameter and $Z(T)$ a normalization factor. The minima are recovered upon slowly decreasing T (‘annealing’) in the limit $T \rightarrow 0$.

In this work, in order to retrieve the individual MCLs as ground states of E , we have performed iterated Metropolis-based annealings to minimize the energy (11) as detailed in the Text

S1. Eventual linear dependencies among the retrieved minima can be resolved by Gaussian elimination to yield an actual non-negative integer basis for the space of MCLs. In case superpositions of independent MCLs (for which $E=0$ as well) are identified as minima of E by Monte Carlo, they can be easily reduced by iteratively subtracting the other independent MCLs found, taking care to maintain the non-negativity constraint for the coefficients k_m .

Step (c): checking completeness. As in [29], we can exploit the connection between (7) and its dual system [21], i.e.

$$\mathbb{S} \mathbf{v} \geq 0, \quad \mathbf{v} \neq \mathbf{0}, \quad v_r \in \mathbb{R} \quad \forall r. \quad (14)$$

The solution spaces of (7) and (14) are linked by the Motzkin theorem of the alternative, which can be stated as follows:

Theorem (Motzkin, 1936). *Consider any arbitrary subset R of rows of \mathbb{S} . Then, either there exists a solution \mathbf{v}^* to system (14) such that all inequalities corresponding to the subset R hold strictly, or system (7) has a solution \mathbf{k}^* , with $k_m^* > 0$ for each $m \in R$.*

In essence, Motzkin’s result guarantees that solutions of (14) verify strict *equalities* for metabolites belonging to MCLs. This is rather intuitive if one interprets strict inequalities in (14) as conditions for metabolite producibility [29,46]. Luckily, a solution of a subset of constraints in (14) with strict *inequalities* can be found very efficiently by relaxation algorithms (e.g. MinOver [47] or Motzkin’s scheme [48]). These classic methods work by correcting iteratively (t being the step) the least unsatisfied constraint, according to the scheme

$$\underline{m}(t) = \arg \min_m \sum_i S_{m,i} v_i(t) \quad (15)$$

$$v_i(t+1) = v_i(t) + \lambda S_{\underline{m}(t),i}, \quad (16)$$

λ being a parameter that can be fixed in different ways, from a constant (as in MinOver [49]) to a quantity proportional to the amount by which the constraint is violated (as in the so-called Motzkin scheme [48]). The above dynamics converges to a solution, if one exists, in polynomial time.

Therefore a simple numerical check to confirm that all MCLs have been found consists in looking for a solution of (14) with strict inequalities for all m ’s remaining after having removed from \mathbb{S} the rows corresponding to metabolites belonging to at least one MCL: when all MCLs have been found, a solution necessarily exists and relaxation converges to it. Further details are reported in the Text S1. This completeness analysis finalizes our protocol.

Materials

We shall apply the method described above to find MCL bases for two reconstructions of *E. coli*’s metabolic networks of rather different sizes, namely iJR904 [4], with $M=761$ chemical species and $N=1074$ reactions, and iAF1260 [50], with $M=1668$ and $N=2381$. These numbers refer to the sizes of the respective stoichiometric matrices including all uptakes but excluding the biomass reaction. Two limiting cases for the choice of the exchange fluxes will be considered. First, we shall analyze MCLs formed in a ‘rich medium’, where all uptake reactions are active. Then, we shall look at the case of ‘minimal medium’, by studying MCLs after having eliminated part of the intakes, while keeping exchange reactions for ca2, fe2, glc-D, h2o, h, k, mg2, mn2, na1, nh4, o2, pi, so4 and zn2. (In the latter case a much larger number of MCLs is to be expected.) We shall see that, while for iAF1260

independent MCLs suffice to generate all conservation laws as linear combinations with non-negative coefficients (in other words, the bound (5) is saturated), the model iJR904 presents one conserved quantity that cannot be expressed as a linear superposition of MCLs with non-negative coefficients.

We have furthermore computed the independent MCLs emerging in 6 tissue-specific reconstructions of human metabolic networks derived from the reactome Recon-2 [32] (bone marrow, breast glandular, heart muscle, hippocampus glial and neuronal and liver hepatocytes), as well as in the entire reactome. The latter case serves mainly to obtain computing times in a worst case (largest reconstruction tested). MCLs for the human networks were obtained using stoichiometric matrices that include all uptakes and exclude the (eventual) biomass reaction.

Results

E. coli iAF1260

Table 1 lists the independent MCLs found for iAF1260 with a ‘rich medium’. They are 38 in total, matching exactly the dimension of the left kernel of the stoichiometric matrix.

20 of them (numbers 1–19 and 32) are formed by a tRNA in two forms: free and bound to its corresponding amino-acid. To have a physical interpretation, we note that if a model possesses a conserved quantity corresponding to a chemical moiety, then that model is closed with respect to that moiety, in the sense that it does not allow for changes in the level of that particular chemical group. In this sense, MCLs based on a tRNA reflect the fact that, in the model where they have been found, the expression of each tRNA is necessarily constant (more precisely, it is assumed to change on time scales longer than those over which metabolite levels equilibrate).

Compounds in MCL 20, arbutin 6-phosphate (arbt6p) and hydroquinone (hqn) only occur in one reaction (arbutin 6-phosphate glucohydrolase: $arbt6p + h_2o \rightarrow g6p + hqn$). From a topological point of view, they represent ‘leaves’ of the reaction network, in the sense that arbt6p is not produced by any reaction while hqn is not consumed by any reaction. The fact that their overall level is invariant is merely due to this peculiar geometric property.

MCL 21 is composed by hydrogen cyanide (cyan) and thiocyanate (tcynt) in their cytoplasmic form. Interestingly, the aggregate concentration of these compounds is conserved despite the fact that, in the rich medium, there are uptakes for both. This is due to the fact that the model lacks reactions that transport the periplasmic species into the cytoplasm. Exactly the same situation holds for the MCLs 22 and 23, formed by dimethyl-sulfide (dms) and -sulfoxide (dmsO), and by thymethylamine (tma) and thymethylamine-N-oxide (tmao), respectively.

MCLs 24–28 express the conservation of the level of lipoproteins (apolipoprotein, disulfide isomerase I and II, disulfide interchange and oxidase). Notice that MCL 28 is the only one to involve periplasmic species exclusively.

MCLs 29–31 describe the invariance of the level of the redox enzymes flavodoxin (fldox), glutaredoxin (grdox) and thioredoxin (trdox).

Compounds in MCLs 33 and 34 are all based on the element selenium, with respect to which the model is closed (i.e. there are no uptakes of selenium-based compounds). We also note from this example that independent MCLs can be overlapping, in the sense that the same compound (sectrna in this case) may belong to different conserved quantities. In such cases, the levels of metabolites in the overlapping groups become effectively coupled, allowing to re-cast the moiety conservation laws associated to the overlapping pools in simpler terms. In the present case, for

Table 1. The 38 independent MCLs found for the network iAF1260.

| MCL ID | Size | Conserved species | Formula |
|--------|------|------------------------------|---|
| 1–19 | 2 | tRNA | alatrna[c] + trnaala[c], argtrna[c] + trnaarg[c], asntrna[c] + trnaasn[c], asptrna[c] + trnaasp[c], cystrna[c] + trnacys[c], glntrna[c] + trnagln[c], glutrna[c] + trnaglu[c], glytrna[c] + trnagly[c], histrna[c] + trnahis[c], iletrna[c] + trnaile[c], leutrna[c] + trnaleu[c], lystrna[c] + trnalys[c], phetrna[c] + trnaphe[c], protrna[c] + trnapro[c], sertrna[c] + trnaser[c], thtrrna[c] + trnathr[c], trptrnatrp[c] + trnatrp[c], tyrtrnatyr[c] + trnatyr[c], valtrnaval[c] + trnaval[c] |
| 20–23 | 2 | missing transport and leaves | arbt6p[c] + hqn[c], cyan[c] + tcynt[c], dms[c] + dmsO[c], tma[c] + tmao[c] |
| 24–28 | 2 | lipoprotein | alpp[p] + lpp[p], dsbaox[p] + dsbard[p], dsbcox[p] + dsbcrd[p], dsbdox[c] + dsbdrd[c], dsbgox[p] + dsbgrd[p] |
| 29–31 | 2 | redox enzymes | fldox[c] + fldrd[c], grdox[c] + grxrd[c], trdox[c] + trdrd[c] |
| 32 | 3 | tRNA | fmettrna[c] + mettrna[c] + trnamet[c] |
| 33–34 | 3 | selenium compounds | sectrna[c] + seln[c] + selnp[c], sectrna[c] + sertrnasec[c] + trnasecys[c] |
| 35 | 3 | biotin | btn[c] + btnso[c] + s[c] |
| 36 | 3 | | 8aonn[c] + amob[c] + pmcoa[c] |
| 37 | 6 | | 8aonn[c] + btn[c] + btnso[c] + dann[c] + dtbt[c] + pmcoa[c] |
| 38 | 53 | ACP | 3haACP[c] + 3hcddec5eACP[c] + 3hcms7eACP[c] + 3hcpalm9eACP[c] + 3hcvac11eACP[c] + 3hddecACP[c] + 3hddecACP[c] + 3hhexACP[c] + 3hmrsACP[c] + 3hoctACP[c] + 3hoctaACP[c] + 3hpalmACP[c] + 3ocdddec5eACP[c] + 3ocms7eACP[c] + 3ocpalm9eACP[c] + 3ocvac11eACP[c] + 3oddecACP[c] + 3oddecACP[c] + 3ohexACP[c] + 3omrsACP[c] + 3ooctACP[c] + 3ooctdACP[c] + 3opalmACP[c] + ACP[c] + acACP[c] + actACP[c] + apoACP[c] + but2eACP[c] + butACP[c] + cddec5eACP[c] + cdec3eACP[c] + dcaACP[c] + ddcaACP[c] + hdeACP[c] + hexACP[c] + malACP[c] + myrsACP[c] + ocACP[c] + ocddaACP[c] + octeACP[c] + palmACP[c] + t3c11vaceACP[c] + t3c5ddeceACP[c] + t3c7mrseACP[c] + t3c9palmeACP[c] + tdddec2eACP[c] + tdeACP[c] + tdec2eACP[c] + thex2eACP[c] + tms2eACP[c] + toct2eACP[c] + toctd2eACP[c] + tpalm2eACP[c] |

The suffixes [c] and [p] indicate the presence of that species in the cytoplasm and periplasm, respectively, in agreement with the compartmentation indicated in the reconstruction.

doi:10.1371/journal.pone.0100750.t001

instance, the fact that *sectrna* is shared by MCLs 33 and 34 corresponds to the conservation of the single quantity $c_{\text{seln}[c]} + c_{\text{selnp}[c]} - c_{\text{sectrnasec}[c]} - c_{\text{trnasecys}[c]}$.

MCL 35 reflects the conservation of the level of biotin, while the sulfur atom is a leaf of the network, appearing only in the biotin synthase reaction.

MCL 36 expresses the invariance of the aggregate level of 8-amino-7-oxononanoate (*8aonn*), S-adenosyl-4-methylthio-2-oxobutanoate (*amob*) and pimeloyl-coa (*pmcoa*), while MCL 37 involves *8aonn*, *pmcoa*, the biotin compounds of pool 35 (*btn*, *btnso*), plus 7,8-diaminononanoate (*dann*) and dethiobiotin (*dtbt*), providing a further instance of overlapping independent pools. At odds with previously described MCLs, these appear lack a clear interpretation in terms of a chemical moiety.

Finally, MCL 38 represents the conservation of the level of acyl carrying protein (ACP).

We can argue that a suitable set of additional uptakes (comprising tRNAs, selenium, disulfide proteins, the aforementioned redox enzymes, biotin, and ACP), together with the missing periplasm-cytosol transport reactions (for cyan, *tma* and *dms*), will render the iAF1260 network completely open, thereby allowing for the possibility that the levels of each of the chemical moieties appearing therein are altered. Eliminating uptakes, on the other hand, will generate additional MCLs. Table 2 reports the 36 additional independent MCLs that occur in iAF1260 in a ‘minimal medium’ containing only *ca2*, *fe2*, *glc-D*, *h2o*, *h*, *k*, *mg2*, *mn2*, *na1*, *nh4*, *o2*, *pi*, *so4* and *zn2* (i.e. by allowing for 14 of the 299 possible uptakes). A close inspection reveals that many of these MCLs emerge from the lack of uptakes for elements like silver (39), cadmium (40), nickel (41), molybdenum (42), cobalt (43), tungsten (44), mercury (46), chloride(47), arsenic (55) and copper (64). A more detailed biochemical analysis is required to interpret the remaining MCLs.

Notice that, while 72 of the MCLs discussed above correspond to solutions of (7) with $k_m \in \{0,1\} \forall m$, MCL 72 has $k_m \in \{0,1,2\} \forall m$ while MCL 73 has $k_m \in \{0,1, \dots, 4\} \forall m$. This shows that, while in general identifying SPCLs cannot be treated as a Boolean problem, the range of values of k_m to be considered in (7) can be relatively small.

E. coli iJR904

For sakes of comparison, in Tables 3 and 4 we report the independent MCLs found in the iJR904 reconstruction of *E. coli*'s metabolism in the ‘rich’ (all uptakes allowed) and ‘minimal’ (defined in the same way as for iAF1260) media, respectively. One can see that, in essence, the MCLs of iJR904 are included among those of iAF1260, with some simplifications. For instance, the pool related to ACP conservation (number 17 in Table 3) is smaller in iJR904 than it is in iAF1260. Notice also that MCL 29 in Table 4 displays two anomalous coefficients $k_m = 50$, due to the effective, non-integer stoichiometry with which the corresponding compounds occur in the reconstruction. When a compound is represented by a small non-integer coefficient in a reaction, solutions of (7) will typically take on large values of k_m .

Considering the ‘rich medium’, it is interesting to note that, even though Table 3 exhausts all of its MCLs (17 in total), the existence of an additional conservation law is revealed by studying the left kernel of the stoichiometric matrix, whose dimension turns out to be 18 rather than 17. The corresponding conserved quantity cannot be expressed as a linear combination of MCLs with non-negative coefficients. In particular, it is formed by the levels of 7 metabolites, with the formula

$$\begin{aligned} & c_{5\text{prdmzb}[c]} + c_{\text{dmbzid}[c]} + c_{\text{rdmbzi}[c]} - \\ & c_{\text{adocbi}[c]} - c_{\text{adocbip}[c]} - c_{\text{agdpbc}[c]} - c_{\text{cbi}[c]}. \end{aligned} \quad (17)$$

Once we move to the ‘minimal medium’, however, the chemical species pertaining to this conserved quantity fall into well defined MCLs, namely numbers 30 and 31 in Table 4. The additional 14 independent MCLs generated by iJR904 in a ‘minimal medium’ suffice to describe all conservation laws for this network.

Human metabolic network reconstructions

Finally we turn our attention to the independent MCLs arising within the human reactome Recon-2 and in six of the tissue-specific networks derived from it [32]. The full details of the MCLs we found are provided as Material S1. To summarize results, the sizes of the bases (number of independent MCLs) and the convergence times of the method (specifically, of the C++ code downloadable from <http://chimera.roma1.infn.it/SYSBIO/>) are reported in Table 5.

We note that if a MCL occurs in Recon-2 and its metabolites are present in a specific subnetwork, then the same MCL will be present in the subnetwork as well. An example is given by the aggregate level of mitochondrial NAD and NADPH, which is conserved in the complete reactome and in all subnetworks we tested. On the other hand, a MCL may be present in a tissue specific network but not in the full reactome, as is the case for the MCL describing the conservation of the sodium cation, which occurs in all subnetworks we tested but not in Recon-2, due to the presence of a sodium uptake in the latter but not in the tissue-specific reconstructions.

Only one of the networks we analyzed presents conservation laws that cannot be derived from MCLs, namely the bone marrow cell metabolic network. In this particular case, the convergence time of the method suffers from the lack of a stopping criterion in terms of the dimension of the kernel, so that verification of completeness by a relaxation dynamics is mandatory. In just two other cases convergence times exceed a few seconds, namely for the entire reactome (whose size is over twice as large as that of any other network we tested) and the hippocampus glial network. In the latter case, a large MCL related to the conservation of coenzyme A is present, whose discovery requires a longer computing time. In the worst case (Recon-2), however, the time for the full procedure to converge and output the basis vectors is just over 3 minutes on an Intel Dual Core at 3.06 GHz.

Finally, we note that the number of MCLs and of metabolites involved therein considerably exceed those found in the *E. coli* reconstructions, even though the network sizes are comparable at least with iAF1260. Considering that a reduced structure of MCLs correlates with larger production capabilities, this suggests that bacterial metabolic networks may be intrinsically designed by evolution to cover a broader spectrum of production profiles than their human counterparts. It will be important to validate this scenario on future, more accurate reconstructions of human metabolism.

Scaling of the number of independent MCLs with the network size

In Figure 1 we display the size of the MCL basis (i.e. the number of independent MCLs) as a function of the network size (M in this plot) for the *E. coli* networks we have considered above as well as for a smaller reconstruction, namely the core matrix of the iAF1260 model [50] (formed by $M = 72$ metabolites that interact through $N = 94$ reactions), both for the ‘rich’ and

Table 2. The 36 additional independent MCLs that are found in iAF1260 in a ‘minimal medium’.

| MCL ID | Size | Formula |
|--------|------|---|
| 39 | 2 | ag[c] + ag[e] |
| 40–47 | 3 | cd2[c] + cd2[e] + cd2[p], ni2[c] + ni2[e] + ni2[p], mobd[c] + mobd[e] + mobd[p], cobalt2[c] + cobalt2[e] + cobalt2[p], tungs[c] + tungs[e] + tungs[p], met-D[c] + met-D[e] + met-D[p], hg2[c] + hg2[e] + hg2[p], cl[c] + cl[e] + cl[p] |
| 48–57 | 4 | betald[c] + glyb[c] + glyb[e] + glyb[p], bbtcoa[c] + gbbtn[c] + gbbtn[e] + gbbtn[p], 4hoxpacd[e] + 4hoxpacd[p] + tym[e] + tym[p], dms[e] + dms[p] + dms[o] + dms[p], cyan[e] + cyan[p] + so3[e] + so3[p], 3sala[c] + so2[c] + so2[e] + so2[p], gdp[e] + gdp[p] + gtp[e] + gtp[p], aso3[c] + aso3[e] + aso3[p] + aso4[c], 34dhpac[e] + 34dhpac[p] + dopa[e] + dopa[p], tma[e] + tma[p] + tmao[e] + tmao[p] |
| 58 | 6 | feoxam-un[c] + feoxam-un[e] + feoxam-un[p] + feoxam[c] + feoxam[e] + feoxam[p] |
| 59 | 6 | cpgn-un[c] + cpgn-un[e] + cpgn-un[p] + cpgn[c] + cpgn[e] + cpgn[p] |
| 60 | 6 | fecrm-un[c] + fecrm-un[e] + fecrm-un[p] + fecrm[c] + fecrm[e] + fecrm[p] |
| 61 | 6 | fe3hox-un[c] + fe3hox-un[e] + fe3hox-un[p] + fe3hox[c] + fe3hox[e] + fe3hox[p] |
| 62 | 6 | arbtn-fe3[c] + arbtn-fe3[e] + arbtn-fe3[p] + arbtn[c] + arbtn[e] + arbtn[p] |
| 63 | 6 | acgal1p[e] + acgal1p[p] + acgal[e] + acgal[p] + udpacgal[e] + udpacgal[p] |
| 64 | 6 | cu2[c] + cu2[e] + cu2[p] + cu[c] + cu[e] + cu[p] |
| 65 | 6 | cyan[e] + cyan[p] + tcynt[e] + tcynt[p] |
| 66 | 6 | chol[c] + chol[e] + chol[p] + g3pc[c] + g3pc[e] + g3pc[p] |
| 67 | 7 | mercppyr[c] + tcynt[c] + tcynt[e] + tcynt[p] + tsul[c] + tsul[e] + tsul[p] |
| 68 | 7 | pac[c] + pacald[c] + pacald[e] + pacald[p] + peamn[e] + peamn[p] + phaccoa[c] |
| 69 | 9 | g3pi[c] + g3pi[e] + g3pi[p] + inost[c] + inost[e] + inost[p] + mi1p-D[c] + minohp[e] + minohp[p] |
| 70 | 9 | 5prdmzbz[c] + adocbl[c] + adocbl[e] + adocbl[p] + cbl1[c] + cbl1[e] + cbl1[p] + dmbzid[c] + rdmbzid[c] |
| 71 | 10 | crnDcoa[c] + crn-D[c] + crn-D[p] + crn[c] + crn[e] + crn[p] + crncoa[c] + ctbt[c] + ctbt[p] + ctbtcoa[c] |
| 72 | 10 | (2) dopa[e] + (2) dopa[p] + (2) h2o2[e] + (2) h2o2[p] + o2s[e] + o2s[p] + (2) peamn[e] + (2) peamn[p] + (2) tym[e] + (2) tym[p] |
| 73 | 11 | aragund[c] + garagund[c] + gfgaragund[c] + (2) o16a2und[p] + (3) o16a3und[p] + (4) o16a4colipa[e] + (4) o16a4colipa[p] + (4) o16a4und[p] + o16aund[c] + o16aund[p] + ragund[c] |
| 74 | 12 | adocbi[c] + adocbi[p] + adocbl[c] + adocbl[e] + adocbl[p] + agdpcbi[c] + cbi[c] + cbi[e] + cbi[p] + cbl1[c] + cbl1[e] + cbl1[p] |

Numbers in parenthesis refer to the values of k_m for the specific metabolites, when different from 1.
doi:10.1371/journal.pone.0100750.t002

‘minimal’ media. The ‘rich medium’ for the *E. coli* core network allows for 20 uptakes, 5 of which (glc-D, o₂, nh₄, pi, h₂o) survive in the ‘minimal medium’. This network is easily seen to present, in both media, 5 MCLs with straightforward biochemical meaning: nad + nadh (nad conservation), nadp + nadph (nadp conservation), q8 + q8h₂ (coenzyme-Q conservation), amp + arp + atp (adenylate moiety conservation) and coa + accoa + succoa (coenzyme-A conservation). It appears that the number of independent MCLs scales approximately linearly with the network size. (A similar study for the human tissue-specific networks is less fruitful, as the network sizes are similar in those cases and indeed the number of independent MCLs retrieved is roughly constant, as shown in the Text S1.) While the investigation of a larger family of

networks is needed to characterize this regularity more thoroughly, it is instructive to analyze the origin of this scaling behaviour. Interestingly, some insight can be obtained from the analysis of random networks.

Consider an ensemble of ‘random metabolic networks’ with N reactions and M compounds, such that each stoichiometric coefficient is chosen randomly and independently with probabilities ($0 < \gamma < 1$)

$$\text{Prob}(S_{mr} = 0) = 1 - \gamma \quad (18)$$

Table 3. The 17 independent MCLs found for the complete network iJR904.

| MCL ID | Size | Formula |
|--------|------|--|
| 1–10 | 2 | trdrd[c] + trdox[c], seln[c] + selnp[c], trnaglu[c] + glutrna[c], dms[c] + dms[o], tmao[c] + tma[c], hqn[c] + arbt6p[c], tcynt[c] + cyan[c], 3dhgulin[c] + 23dogulin[c], idp[c] + itp[c], acon_T[c] + aconm[c] |
| 11–14 | 3 | ctbt[c] + gbbtn[c] + crn[c], g3pi[c] + inost[c] + mi1p_D[c], 8aonn[c] + amob[c] + pmcoa[c], bbtcoa[c] + crncoa[c] + ctbtcoa[c] |
| 15 | 4 | pacald[c] + peamn[c] + pac[c] + phaccoa[c] |
| 16 | 6 | pmcoa[c] + 8aonn[c] + dann[c] + dtbt[c] + btn[c] + btnso[c] |
| 17 | 12 | apoACP[c] + acACP[c] + actACP[c] + ACP[c] + malACP[c] + ddcaACP[c] + octeACP[c] + myrsACP[c] + palmACP[c] + hdeACP[c] + tdeACP[c] + 3hmsrACP[c] |

The suffix [c] indicates that the compound occurs in the cytoplasm.
doi:10.1371/journal.pone.0100750.t003

Table 4. The 14 additional independent MCLs that are found in iJR904 in a “minimal medium”.

| Pool ID | Size | Formula |
|---------|------|---|
| 18–23 | 2 | fuc1p_L[c] + fuc1p_L[e], dms0[e] + dms[e], nad[e] + amp[e], met_D[e] + met_D[c], tmao[e] + tma[e], gbbtn[e] + crn[e] |
| 24–27 | 3 | glyb[c] + betald[c] + glyb[e], taur[e] + taur[c] + aacald[c], gbbtn[c] + gbbtn[e] + bbtcoa[c], tsul[e] + tsul[c] + tcynt[c] |
| 28 | 5 | ctbtcoa[c] + ctbt[c] + crncoa[c] + crn[c] + crn[e] |
| 29 | 5 | g3pc[c] + chol[c] + (50) pc_EC[c] + (50) agpc_EC[c] + chol[e] |
| 30 | 6 | rdmbzi[c] + adocbl[c] + cbl1[c] + cbl1[e] + 5prdmzbz[c] + dmbzid[c] |
| 31 | 7 | adocbip[c] + agdpcbi[c] + adocbl[c] + cbl1[c] + cbl1[e] + adocbi[c] + cbi[c] |

Numbers in parenthesis refer to the values of k_m for the specific metabolites, when different from 1.
doi:10.1371/journal.pone.0100750.t004

$$\text{Prob}(S_{mr} = 1) = \text{Prob}(S_{mr} = -1) = \gamma/2. \quad (19)$$

The parameter γ rules the average connectivity of the network. In particular, we will assume that $\gamma = 2c/N$ (with c a constant), and consider the limit $N, M \rightarrow \infty$, keeping a fixed ratio $\alpha = N/M$. In this limit, the above model generates sparse stoichiometric matrices with Poisson distribution for the in- and out-degrees, with average values $\langle d_{in}^m \rangle = \langle d_{out}^m \rangle = c$ for metabolites and $\langle d_{in}^r \rangle = \langle d_{out}^r \rangle = c/\alpha$ for reactions, respectively. (In real networks, the degree distribution of metabolites is known to have heavy tails due to the presence of ubiquitous compounds like water, ATP, etc. whose connectivities typically grow with the network size. On the other hand, the degree distribution of the remaining metabolites follows a Poissonian law to a good approximation.) By definition, the overall number of MCLs of size n (i.e. involving n chemical species) is given by

$$\mathcal{N}_n = \sum_{\mathbf{k}: \|\mathbf{k}\|=n} \prod_{r=1}^N \delta \left(\sum_{m=1}^M k_m S_{mr} \right), \quad (20)$$

where $\delta(x)$ denotes Dirac's δ -function, we assume $k_m \in \{0, 1\}$ for sakes of simplicity for each m , and $\|\mathbf{k}\| = \sum_m k_m$. \mathcal{N}_n as defined above however includes all linear combinations of independent MCLs that produce a new MCL of size n . To obtain the number

of independent MCLs, one should subtract from \mathcal{N}_n the contributions due to superpositions of smaller pools. For instance, all distinct pairs of pools of size 1 would contribute to \mathcal{N}_2 as well, so that the number of independent pools of size 2 is given by

$$\mathcal{N}_2^{\text{irr}} = \mathcal{N}_2 - \frac{\mathcal{N}_1(\mathcal{N}_1 - 1)}{2}. \quad (21)$$

Expression (20) furthermore depends on the particular network being examined. We shall focus on its average over the entire ensemble. Writing the δ -function as $\delta(x) = \frac{1}{2\pi} \int_0^{2\pi} \exp(ix\phi) d\phi$, summing over k_m 's and averaging over the stoichiometry one finds

$$\langle \mathcal{N}_n \rangle = \binom{M}{n} \left[\frac{1}{2\pi} \int_0^{2\pi} (1 - \gamma + \gamma \cos \phi)^n d\phi \right]^N. \quad (22)$$

Expanding the integrand and noting that

$$\frac{1}{2\pi} \int_0^{2\pi} (\cos \phi)^k d\phi = \begin{cases} 2^{-k} \binom{k}{k/2} & \text{if } k \text{ is even} \\ 0 & \text{otherwise} \end{cases}, \quad (23)$$

one finally obtains

Table 5. Summary of the number of independent MCLs, of the overall number of metabolites included in at least one MCL basis element and of the convergence times of our algorithm for the networks being examined.

| Network | N | M | # MCLs | # metabolites in MCLs | convergence time (s) |
|----------------------|------|------|--------|-----------------------|----------------------|
| E. Coli core | 94 | 72 | 5 | 12 | $< 10^{-6}$ |
| E. Coli iJR904 | 1074 | 761 | 17 | 52 | 5.47 |
| E. Coli iAF1260 | 2381 | 1668 | 38 | 131 | 2.86 |
| Bone_Marrow | 2274 | 1579 | 85 | 294 | 78 |
| Breast_glandular | 2484 | 1716 | 88 | 279 | 1.7 |
| Heart_muscle | 2692 | 1929 | 104 | 346 | 2.1 |
| Hippocampus_glial | 1576 | 1033 | 107 | 414 | 49.21 |
| Hippocampus_neuronal | 2303 | 1588 | 94 | 275 | 1.47 |
| Liver_hepatoocytes | 3040 | 2166 | 95 | 309 | 2.89 |
| Recon 2 | 7440 | 5063 | 397 | 1135 | 216 |

Convergence times were measured for the C++ code that can be downloaded from <http://chimera.roma1.infn.it/SYSBIO/> on an Intel Dual Core running at 3.06 GHz. N and M denote, respectively, the numbers of reactions and metabolites that characterize the reconstructions.
doi:10.1371/journal.pone.0100750.t005

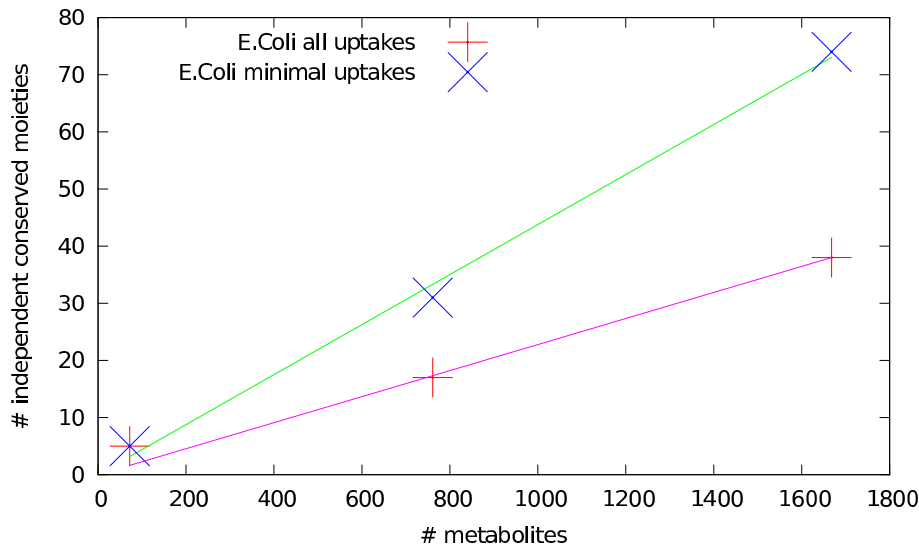


Figure 1. Scaling of the number of independent MCLs with the network size. Size of the MCL basis as a function of the number of metabolites (M) for three *E. coli* metabolic network reconstructions in ‘rich’ (all uptakes active) and ‘minimal’ media. doi:10.1371/journal.pone.0100750.g001

$$\langle \mathcal{N}_n \rangle = \binom{M}{n} (1-\gamma)^{Nn} \left[\sum_{k \text{ even}} \binom{n}{k} \binom{k}{k/2} \frac{\gamma^k}{2^k (1-\gamma)^k} \right]^N, \quad (24)$$

which can be evaluated in the limit $N \rightarrow \infty$. For $n=2$, keeping only the leading-order terms in M and approximating $\langle \mathcal{N}_1^2 \rangle \simeq \langle \mathcal{N}_1 \rangle^2$ in (21), one gets

$$\langle \mathcal{N}_2^{\text{irr}} \rangle \simeq \frac{M}{2} (e^{-2c} - e^{-4c}). \quad (25)$$

For the networks being examined, once the most connected compounds are removed, one finds $c \simeq 1.6$, leading to $\langle \mathcal{N}_2^{\text{irr}} \rangle \simeq 2, 15, 32$ for the *E. coli* core, iJR904 and iAF1260 models, respectively (considering a ‘rich medium’). This should be compared with the actual numbers of independent pools of size 2 we found, namely 3, 10 and 31 respectively. (Similar results can be obtained, with more work, for larger values of n .)

It is now straightforward to show that the size B of the pool basis scales linearly with M . Upon summing (24) over n , the total number of pools $\mathcal{N}_{\text{tot}} = \sum_n \langle \mathcal{N}_n \rangle$ is seen to satisfy

$$(1 + e^{-2c})^M \leq \mathcal{N}_{\text{tot}} \leq 2^M. \quad (26)$$

In other terms, there exists a number $z \in [1, 2]$ such that $\mathcal{N}_{\text{tot}} = z^M$. On the other hand, assuming for simplicity that pools in the basis are non-overlapping, one has $\mathcal{N}_{\text{tot}} = 2^B$, from which we get $B = M \log_2 z$, i.e. a linear scaling with M , in agreement with the behavior displayed in Figure 1. Therefore, despite the coarse way in which it approximates the considerably more structured real metabolic networks, this ensemble of random networks does provide useful hints about the origin of the scaling behavior observed in cellular networks.

Discussion

Conservation laws described by the left kernel of the stoichiometric matrix \mathbb{S} take on a specific biochemical significance when

the coefficients involved in their definition are non-negative integers, in which case they typically describe the conservation of a particular molecular moiety. Moiety conservation laws have been shown to have relevant biotechnological or medical implications [51], and are bound to play a key role in understanding the dynamics of intracellular reaction networks. Indeed, conservation relationships, as specific dependencies among variables, allow in principle to reduce the number of degrees of freedom, thereby speeding up dynamical simulations. Unluckily, though, dynamical approaches are still largely prevented from limited knowledge of kinetic constants and reaction mechanisms. Identifying the independent conserved moieties embedded in a given \mathbb{S} , however, requires solving the hard constraint-satisfaction problem of finding all integer, non-negative, solutions to a linear system of equations defined by the network’s input-output relationships and corresponding roughly to the maximal conserved moieties introduced in [25]. Methods to tackle this issue on small networks are available and have been employed before. For the network sizes relevant in metabolic modeling, though, the *a priori* search space of the problem is huge and exact methods are doomed to fail because of exceeding computational costs. It is crucial to stress that intractability arises even in presence of a small number of independent MCLs from the fact that retrieving them by a deterministic method would require an exhaustive search through an exponentially large number of candidate solutions. (On the other hand, it is clear that problems with an exponential number of solutions are not necessarily hard to solve.)

Luckily, powerful heuristics to tackle this type of problems has been developed in the last decade at the interface between statistical mechanics and computer science. Here, we have constructed and applied a technique that allows to obtain full information about the independent MCLs associated to a large-scale stoichiometric matrix \mathbb{S} in reasonable computing times (a few seconds for genome-scale metabolic networks). In particular, we combine different approaches (message passing, Monte Carlo, and relaxation algorithms) in order to construct a basis for MCLs through which all conserved metabolite pools (i.e. all semi-positive conservation laws) can be described. In short, we first prune irrelevant variables, then extract individual MCLs from the

remaining ones, and finally validate our results for completeness of the MCL basis thus obtained. We have analyzed the structure of the MCLs emerging in two large-scale reconstructions of the metabolism of *E. coli* and in the human reactome reconstruction Recon-2, as well as in six tissue-specific subnetworks. In most cases, independent MCLs either display a simple biochemical meaning or their origin can be clearly traced back to properties of the reconstruction. In some cases, however, it is difficult to identify a precise molecular rationale for the groups we obtain. We note however that cofactors like ATP, ADP, AMP, NADH, NADPH, FADH₂, etc. do not generically appear in conservation relationships in genome-scale reconstructions. More generally, we have suggested the existence of a linear relation between the number of independent MCLs and the network size, validating it in data and by an analytical calculation for ‘random metabolic networks’, although more work will be needed to characterize this picture more thoroughly.

The foremost advantage of our stochastic method is provided by the limited computing times with respect to the previously defined deterministic methods, which require exponentially large CPU costs in the worst case. It is anyway worth to comment briefly about the appropriateness of the techniques we employ to find independent MCLs. Concerning the Monte Carlo method, the algorithm is a Markov chain verifying the detailed balance condition with respect to the measure (13). Since the states are connected, this condition implies that the chain is ergodic [52]. In very large networks the method may however suffer from effective breakdowns of ergodicity due to exceeding relaxation times. We have however not encountered phenomena of this type on the genome-scale networks we analyzed. On the other hand, the MP protocol we use is formally guaranteed to converge only on tree-like networks, which is a potential drawback. We have however noted that the list of metabolites belonging to at least one MCL can be also computed in other ways, e.g. by analyzing the left kernel of the stoichiometric matrix. This is indeed done explicitly in the C++ code that can be downloaded (together with the test case given by the iAF1260 reconstruction of *E. coli*’s metabolic network) from <http://chimera.roma1.infn.it/SYSBIO/>, where the overall method we propose is implemented in an automatic way with the only input of a stoichiometric matrix. The fact that MP and kernel analysis provide the same results on each of the 9 networks we tested very strongly suggests that the convergence problems of which MP may suffer on metabolic networks may be less severe than one would have expected. This only confirms the indications obtained from previous MP-based studies of metabolic networks [18]. Unfortunately, MP algorithms are hard to automatize. The possibility to obtain more thorough and potentially useful information through this heuristics (e.g. about the statistics of the vector \mathbf{k} over the solution space) still represents a very high incentive toward their use in our view. For instance, it may be possible to replace the Monte Carlo step by complementing MP with a decimation procedure [52,53], thus allowing to map out the full set of independent MCLs of a large, genome-scale metabolic network by MP alone, something that would be unfeasible by Monte Carlo.

References

- Jeong H, Tombor B, Albert R, Oltvai Z, Barabasi AL (2000) The large-scale organization of metabolic networks. *Nature* 407: 651–654.
- Fell D, Wagner A (2000) The small world of metabolism. *Nature Biotech* 18: 1121–1122.
- Dongxiao Z, Zhaohui S (2005) Structural comparison of metabolic networks in selected single cell organisms. *BMC Bioinformatics* 6: 8.
- Reed J, Vo T, Schilling C, Palsson B (2003) An expanded genome-scale model of *Escherichia coli* k-12 (iJR904 GSM/GPR). *Genome Biol* 4: R54.
- Palsson B (2006) *Systems biology: properties of reconstructed networks*. Cambridge (UK): Cambridge University Press.
- Almaas E, Kovacs B, Vicsek T, Oltvai Z, Barabasi AL (2004) Global organization of metabolic fluxes in the bacterium *Escherichia coli*. *Nature* 427: 839–843.
- Segré D, Vitkup D, Church G (2002) Analysis of optimality in natural and perturbed metabolic networks. *Proc Natl Acad Sci USA* 99: 15112–15117.

Besides their importance for dynamical modeling widely discussed in the literature [22,26,27,51], MCLs (or, more generally, the SPCLs that they generate) provide crucial indications concerning how a cell will respond to a perturbation that e.g. increases the level of a particular chemical species. The manner in which that perturbation propagates is indeed constrained by the map of MCLs. In addition, results obtained here can improve producibility predictions [19]. The technique we have presented is successful in large, genome-scale models, and applicability to other organisms is straightforward. More interestingly, however, it may represent a general protocol by which different stoichiometry-based problems that are inherently integer programming ones can be tackled. For instance, a similar approach may form the basis of a method that will tackle the potentially harder problem of computing all extreme pathways of a reaction network at genome-scale resolution [13]. The main difference with the case discussed here is that, while computing the independent MCLs of a genome-scale metabolic network means finding a non-negative integer basis for the SPCLs described by the left kernel of the stoichiometric matrix, extreme pathways form an outright Hilbert basis of the right kernel of the stoichiometric matrix, and the number of elements of a Hilbert basis can be much larger than that of a simple basis. Nevertheless, the existence of useful upper bounds [54] and the excellent performance of the algorithm we introduce may combine to provide cost-effective heuristics for this problem as well. We finally point out that the general issue of producibility in metabolic networks goes beyond purely stoichiometric (mass) constraints and it should include thermodynamics constraints as well. This can be addressed with similar computational techniques, an aspect that we will leave for further studies.

Supporting Information

Text S1 Detailed description of the methods, description of the C++ code downloadable (with a text case) from <http://chimera.roma1.infn.it/SYSBIO/>, and scaling of the number of independent MCLs with the network size in human metabolic reconstructions.
(PDF)

Material S1 Independent MCLs found in the human reactome Recon-2 as well as in the six tissue-specific networks tested.
(GZ)

Acknowledgments

The authors thank A. Braunstein for sharing with us the implementation of the MP algorithm, and for many relevant discussions.

Author Contributions

Conceived and designed the experiments: ADM DDM RM AP. Performed the experiments: ADM DDM RM AP. Analyzed the data: ADM DDM RM AP. Contributed reagents/materials/analysis tools: ADM DDM RM AP. Wrote the paper: ADM DDM RM AP.

8. Joyce A, Palsson B (2008) Predicting gene essentiality using genome-scale in silico models. *Methods Mol Biol* 416: 433–457.
9. Schellenberger J, Que R, Fleming R, Thiele I, Orth J, et al. (2011) Quantitative prediction of cellular metabolism with constraint-based models: the cobra toolbox v2.0. *Nature Protocols* 6: 1290–1307.
10. Heinrich R, Schuster S (1996) *The Regulation of Cellular Systems*. Berlin: Springer.
11. Beard D, Qian H (2008) *Chemical biophysics*. Cambridge (UK): Cambridge University Press.
12. Behre J, de Figueiredo L, Schuster S, Kaleta C (2012) Detecting structural invariants in biological reaction networks. In: *Bacterial Molecular Networks: Methods and Protocols (Methods in Molecular Biology, vol. 804)*. pp. 377–407.
13. Yeung M, Thiele I, Palsson B (2007) Estimation of the number of extreme pathways for metabolic networks. *BMC Bioinformatics* 8: 363.
14. Papin J, Price N, Edwards J, Palsson B (2002) The genome-scale metabolic extreme pathway structure in haemophilus influenzae shows significant network redundancy. *J Theor Biol* 215: 67–82.
15. Schuster S, Dandekar T, Fell D (1999) Detection of elementary ux modes in biochemical networks: a promising tool for pathway analysis and metabolic engineering. *Trends Biotechnol* 17: 53–60.
16. Wiback S, Famili I, Greenberg H, Palsson B (2004) Monte carlo sampling can be used to determine the size and shape of the steady-state ux space. *J Theor Biol* 228: 437–447.
17. Price N, Schellenberger J, Palsson B (2004) Uniform sampling of steady-state ux spaces: means to design experiments and to interpret enzymopathies. *Biophys J* 87: 2172–2186.
18. Braunstein A, Mulet R, Pagnani A (2008) Estimating the size of the solution space of metabolic networks. *BMC Bioinformatics* 9: 240.
19. Martelli C, De Martino A, Marinari E, Marsili M, Perez Castillo I (2009) Identifying essential genes in escherichia coli from a metabolic optimization principle. *Proc Nat Acad Sci USA* 106: 2607–2611.
20. Thiele I, Price N, Vo T, Palsson B (2005) Candidate metabolic network states in human mitochondria. impact of diabetes, ischemia, and diet. *J Biol Chem* 280: 11683–11695.
21. Schuster S, Höfer T (1991) Determining all extreme semi-positive conservation relations in chemical reaction systems: a test criterion for conservativity. *J Chem Soc Faraday Transac* 87: 2561–2566.
22. Famili I, Palsson B (2003) The convex basis of the left null space of the stoichiometric matrix leads to the definition of metabolically meaningful pools. *Biophys J* 85: 16–26.
23. Papadimitrou C, Steiglitz K (2000) *Combinatorial optimization: algorithms and complexity*. Dover Publications Inc.
24. Conti P, Traverso C (1991) Buchberger algorithm and integer programming. In: *Lectures Notes in Computer Science Vol. 539*. Berlin: Springer, pp. 130–139.
25. Schuster S, Hilgetag C (1995) What information about the conserved-moiety structure of chemical reaction systems can be derived from their stoichiometry? *J Phys Chem* 99: 8017–8023.
26. Vallabhajosyula R, Chickarmane V, Sauro H (2006) Conservation analysis of large biochemical networks. *Bioinformatics* 22: 346–353.
27. Sauro H, Ingalls B (2004) Conservation analysis in biochemical networks: computational issues for software writers. *Biophys Chem* 109: 1–15.
28. Nikolaev E, Burgard A, Maranas C (2005) Elucidation and structural analysis of conserved pools for genome-scale metabolic reconstructions. *Biophys J* 88: 37–49.
29. Imielinski M, Belta C, Rubin H, Halász A (2006) Systematic analysis of conservation relations in escherichia coli genome-scale metabolic network reveals novel growth media. *Biophys J* 90: 2659–2672.
30. Gevorgyan A, Poolman M, Fell D (2008) Detection of stoichiometric inconsistencies in bimolecular models. *Bioinformatics* 24: 2245–2251.
31. Koch I (2010) Petri nets: A mathematical formalism to analyze chemical reaction networks. *Molecular Informatics* 29: 838–843.
32. Thiele I, Swainston N, Fleming RMT, Hoppe A, Sahoo S, et al. (2013) A community-driven global reconstruction of human metabolism. *Nature Biotechnol* 31: 419–425.
33. Henk M, Weismantel R (1997) On Hilbert bases of polyhedral cones. *Results Math* 32: 298–303.
34. Coleman T, Pothén A (1986) The null space problem I. Complexity. *SIAM J Alg Discr Meth* 7: 527–537.
35. Contejean E, Devic H (1994) An efficient incremental algorithm for solving systems of linear Diophantine equations. *Inform & Comput* 113: 143–172.
36. Pasechnik V (2001) On computing the Hilbert bases via the Elliott-MacMahon algorithm. *Theor Comp Sci* 263: 37–46.
37. Braunstein A, Mezard M, Zecchina R (2005) Survey propagation: an algorithm for satisfiability. *Random Struct Algor* 27: 201–226.
38. Baldassi C, Braunstein A, Brunel N, Zecchina R (2007) Efficient supervised learning in networks with binary synapses. *Proc Nat Acad Sci USA* 104: 11079–11084.
39. Mulet R, Pagnani A, Weigt M, Zecchina R (2002) Coloring random graphs. *Phys Rev Lett* 89: 268701.
40. Pearl J (1982) Reverend bayes on inference engines: A distributed hierarchical approach. In: *Proc. AAAI Nat. Conf. AI (Pittsburgh, PA)*. pp. 133–136.
41. Kim J, Pearl J (1983) A computational model for causal and diagnostic reasoning in inference systems. In: *Proceedings IJCAI-83 (Karlsruhe, Germany)*. pp. 190–193.
42. Mezard M, Montanari A (2009) *Information, physics, and computation*. Oxford University Press.
43. Yedidia JS, Freeman WT, Weiss Y (2000) Generalized belief propagation. In: *Neural Information Processing Systems 13*. MIT Press, pp. 689–695.
44. Kschischang F, Frey B, Loeliger H (2001) Factor graphs and the sum-product algorithm. *IEEE Transactions on Information Theory* 47: 498–519.
45. Krauth W (1998) Introduction to monte carlo algorithms. *Advances in Computer Simulations* 501: 1–35.
46. Imielinski M, Belta C, Rubin H, Halász A (2005) Investigating metabolite essentiality through genome-scale analysis of escherichia coli production capabilities. *Bioinformatics* 12: 2008–2016.
47. De Martino A, Martelli C, Monasson R, Perez Castillo I (2007) Von Neumann's expanding model on random graphs. *JSTAT* 2007: P05012.
48. Schrijver A (1986) *Theory of linear and integer programming*. Chichester: Wiley.
49. Krauth W, Mezard M (1987) Learning algorithms with optimal stability in neural networks. *J Phys A: Math Gen* 20: L745–L752.
50. Feist A, Henry C, Reed J, Krummenacker M, Joyce A, et al. (2007) A genome-scale metabolic reconstruction for escherichia coli K-12 MG1655 that accounts for 1260 ORFs and thermodynamic information. *Mol Sys Biol* 3: 121.
51. Bakker B, Michels P, Opperdoes F, Westerhoff H (1999) What controls glycolysis in bloodstream form trypanosoma brucei? *J Biol Chem* 274: 14551–14559.
52. Mezard M, Parisi G, Zecchina R (2002) Analytic and algorithmic solution of random satisfiability problems. *Science* 297: 812–815.
53. Ricci Tersenghi F, Semerjian G (2009) On the cavity method for decimated random constraint satisfaction problems and the analysis of belief propagation guided decimation algorithms. *JSTAT* 2009: P09001.
54. Eisenbrand F, Shmonin G (2006) Caratheodory bounds for integer cones. *Operations Research Letters* 34: 564–568.